Pramana – J. Phys. (2018) 90:15
https://doi.org/10.1007/s12043-017-1503-z

Dipole and spin-dipole strength distributions in ^{124,126,128,130}Te isotopes

NECLA CAKMAK[1], SADIYE CAKMAK[2], CEVAD SELAM[3] and SERDAR UNLU[4,*]

[1]Department of Physics, Karabuk University, Karabuk, Turkey
[2]Department of Physics, Eskisehir Osmangazi University, Eskisehir, Turkey
[3]Department of Physics, Mus Alparslan University, Mus, Turkey
[4]Department of Physics, Mehmet Akif Ersoy University, Burdur, Turkey
*Corresponding author. E-mail: serdarunlu@mehmetakif.edu.tr

MS received 23 May 2017; revised 27 August 2017; accepted 29 August 2017; published online 3 January 2018

Abstract. We try to present the structure of 1^- excitations in open-shell ^{124,126,128,130}Te isotopes. Electric dipole states are investigated within a translational and Galilean invariant model. Also, a theoretical description of charge-conserving spin-dipole 1^- excitations is presented for the same isotopes. The energy spectra for both kinds of excitations are analysed in detail. Furthermore, a comparison of the calculated cross-sections and energies with the available experimental data is given.

Keywords. Translational and Galilean invariance; charge-conserving spin dipole excitations.

PACS Nos **21.60.Jz; 23.40.−s**

1. Introduction

The study of giant multipole transitions is very important in understanding the excitation modes of atomic nuclei. The experimental or theoretical investigation of the electromagnetic transitions between nuclear levels provides useful information about the nuclear structure [1]. Electric dipole (E1) resonance has been the subject of many experimental and theoretical studies. The excited 1^- modes in atomic nuclei play significant roles in testing nuclear structure theories. However, these excitation modes can also be studied by means of spin-dipole transitions ($\Delta L = 1$, $\Delta S = 1$).

Charge-exchange spin-dipole transitions were investigated experimentally by (p,n) or (n,p) and $(^3\mathrm{He},t)$ reactions [2–12]. Theoretically, these transitions for double magic ^{40,48}Ca, ^{90}Zr and ^{208}Pb nuclei were analysed within Tamm-Dancoff approximation [13,14] and random phase approximation methods [14–18]. Nevertheless, there is not enough calculation to analyse the charge-conserving spin-dipole decay mode. There have been some experimental attempts for spin-dipole excitation modes by using (p, p') reactions [19,20]. Cross-sections in the $^{16}\mathrm{O}(p, p')$ reactions at 392 MeV were measured at several angles between $\theta = 0$ and 14 and the giant resonances in the energy region of 19–27 MeV were found to be predominantly excited by $\Delta L = 1$ transition [19]. Also, the angular distributions of double differential cross-section were measured for $^{40}\mathrm{Ca}(p, p')$ reaction at 319 MeV [20]. The spin-dipole resonance has a total measured strength which is larger than that predicted by the energy-weighted sum rule and is located around 20 MeV.

The experimental results for ^{16}O are reasonably explained by distorted wave approximation calculations with the shell model wave functions [19]. As is well known, quasiparticle random phase approximation (QRPA) is a powerful tool to explain the collective decay modes for open shell nuclei. According to the approximation, a suitable effective interaction potential must be added as a perturbation to the mean field Hamiltonian. It is also well known that the exact symmetry properties of total nucleus Hamiltonian are violated in the mean field level of approximation. One of these symmetry properties is the translational invariance of Hamiltonian. The restoration of broken translational invariance plays a crucial role to understand the 1^- excitations in even–even nuclei [21]. The restoration of this symmetry violation is enough to study E1 excitation modes in double magic nuclei. However, the pairing correlations which have to be considered for open shell nuclei lead to extra symmetry violations. Thus, the broken Galilean

invariance of pairing interaction has a significant effect on the E1 excitation modes in the open shell nuclei. Hence, the restoration of broken Galilean invariance of pairing interaction becomes important in the study of E1 transitions. Pyatov's restoration method is an efficient way to restore the symmetry violations stemming from the mean field approximation [22–31]. According to this method, the effective interaction potential is included in such a way that the broken symmetry property is restored. The dipole excitations in some magic nuclei were described using the self-consistent translational invariant model with separable effective interaction and with the account of the one-particle continuum [32]. The electric dipole excitations in deformed nuclei were investigated using Pyatov's method within the framework of QRPA method [33–36].

The present work contains an application of Pyatov's method for the study of electric dipole 1^- excitations in ^{124,126,128,130}Te isotopes. Moreover, charge-conserving spin-dipole 1^- excitations in the same isotopes are investigated within QRPA method. Thus, a theoretical analysis of the spin-dipole 1^- excitations in some Te isotopes is presented by using a microscopic approach. In §2, a summary of the mathematical formalism is given. A detailed analysis of the calculated strength distributions and a comparison of the calculated results with available experimental data are given in §3. Conclusions and final remarks are presented in §4.

2. Theoretical formalism

It is well known that the single-particle model is not successful in explaining collective excitation modes in nuclei due to the exclusion of the effective interactions between nucleons. Hence, perturbative approaches are needed to explain these decay modes. In QRPA, the corresponding effective Hamiltonian for the excitation modes under consideration is added to the mean field Hamiltonian and the energies, wave functions of these modes are obtained. The effective Hamiltonian can be defined as a schematic residual interaction containing at least one free parameter. However, the effective nucleon–nucleon interaction can also be determined in such a way that the broken symmetry properties in the mean field approximation can be restored. In Pyatov's restoration method, the corresponding effective interaction Hamiltonian is added to the single-particle Hamiltonian as a perturbation and the effective interaction constant is obtained in a self-consistent way. The E1 excitation modes in open shell nuclei are sensitive to the violations in translational and Galilean invariances. Nevertheless, the spin-dipole decay mode is not related to any exact symmetry of nuclear Hamiltonian. Therefore, this decay mode can be searched within the schematic residual interaction method.

2.1 *Electric dipole transitions*

The model Hamiltonian which produces the E1 excitations in spherical nuclei is defined as follows:

$$H = H_{\rm sqp} + h_0 + h_\Delta + W_1, \tag{1}$$

where $H_{\rm sqp}$ is the single quasiparticle Hamiltonian in a spherical symmetric average field with the pairing forces written in the following form:

$$H_{\rm sqp} = \sum_{jm} \varepsilon_j(\tau)\alpha^\dagger_{jm}(\tau)\alpha_{jm}(\tau), \quad \tau = n, p.$$

Here, ε_j is the single quasiparticle energy and $\alpha^\dagger_{jm}(\alpha_{jm})$ is a quasiparticle creation (annihilation) operator. The broken translational invariance in the mean field approximation is restored using a separable isoscalar effective interaction as [22]

$$h_0 = -\sum_{\mu=0,\pm1} \frac{1}{2\gamma_\mu}[H_{\rm sqp}, P_\mu]^\dagger[H_{\rm sqp}, P_\mu], \tag{2}$$

where P_μ is the spherical component of the linear momentum. We also add a new term to restore the broken Galilean invariance of the pairing interaction as follows [22]:

$$h_\Delta = -\frac{1}{2\beta}\sum_{\mu=0,\pm1}[V_\Delta, R_\mu]^\dagger[V_\Delta, R_\mu]. \tag{3}$$

The pairing field is defined as $V_\Delta = -\frac{\Delta}{2}(\Gamma^\dagger + \Gamma)$ [37], and where $\Gamma = \sum_{jm}(-1)^{j-m}a_{j,-m}a_{jm}$, Δ is the energy gap. The effective interaction parameters are determined from the double commutators in the following form:

$$\gamma_\mu = \langle 0|[P^\dagger_\mu, [H_{\rm sqp}, P_\mu]]|0\rangle, \tag{4}$$

$$\beta = \langle 0|[R^\dagger_\mu, [V_\Delta, R_\mu]]|0\rangle, \tag{5}$$

where $R_\mu = \sum_{k=1}^{A} r_k Y_{lm}(\theta_k, \varphi_k)$ is the centre of mass (c.m.) coordinate of the nucleus. In eq. (1), the term W_1 corresponds to the coherent isovector dipole vibrations of protons and neutrons, the c.m. of the nucleus being at rest. In the case of translation invariant dipole–dipole interaction, the isovector interaction has the following form:

$$W_1 = \frac{3}{2\pi}\chi_1\left(\frac{NZ}{A}\right)^2(\vec{R}_n - \vec{R}_p)^2, \tag{6}$$

where χ_1 denotes an isovector dipole–dipole interaction constant and $\vec{R}_n$, $\vec{R}_p$ are the c.m. coordinate vectors of the neutron and proton systems, respectively.

2.2 *Spin-dipole transitions*

The model Hamiltonian for charge-conserving spin-dipole 1^- excitations is described as follows:

$$H = H_{\text{sqp}} + h_{\text{SD}}. \tag{7}$$

The corresponding effective interaction for these excitations can be defined in a schematic separable form [38] as below:

$$h_{\text{SD}} = -\frac{\chi_0}{2}\sum_{\mu,\tau} S^\dagger_\mu(\tau)S_\mu(\tau) - \chi_1\sum_\mu [S^\dagger_\mu(p)S_\mu(p) + S^\dagger_\mu(n)S_\mu(n)], \tag{8}$$

where S_μ is the spin-dipole transition operator which is given as

$$S_\mu = \sum_{j_1 j_2}\frac{\langle j_2 \| r[Y_1\times\sigma]_1 \| j_1\rangle}{\sqrt{2j_2+1}} \times \sum_{m_1 m_2}\langle j_1 m_1 1\mu \mid j_2 m_2\rangle a^\dagger_{j_2 m_2}a_{j_1 m_1}.$$

The charge-conserving QRPA procedure is applied for both electric dipole ($\Delta S = 0$) and spin-dipole ($\Delta S = 1$) excitations. The energies and wave functions for both excitations are obtained by solving the equation of motion in the following form:

$$[H, Q^\dagger_i(\mu)]|0\rangle = \omega_i Q^\dagger_i(\mu)|0\rangle, \tag{9}$$

where ω_i represents the energies of the excited states. The excited 1^- states are represented by a phonon creation operator in the following form:

$$Q^\dagger_i(\mu)|0\rangle = \sum_{j_1 j_2}[\psi^i_{j_1 j_2}A^\dagger_{j_1 j_2}(\mu) - (-1)^{1-\mu}\varphi^i_{j_1 j_2}A_{j_1 j_2}(-\mu)]|0\rangle,$$

where $\psi^i_{j_1 j_2}$ and $\varphi^i_{j_1 j_2}$ are the forward and backward amplitudes, respectively. $A^\dagger_{j_1 j_2}$ ($A_{j_1 j_2}$) are the quasiboson creation (annihilation) operators. The nuclear matrix element for both electromagnetic transitions is determined from the following equation:

$$M^i(0^+_{\text{g.s.}} \to 1^-) = \langle 1^-_i|\widehat{S_\mu}|0^+_{\text{g.s.}}\rangle.$$

The cross-section and energy-weighted cross-sections for dipole photoexcitations [22] are calculated as

$$\sigma_n = \frac{16\pi^3}{9}\frac{e^2}{\hbar c}\sum_i \omega_i^{n+1}B(\text{E1}, 0^+ \to 1^-_i). \tag{10}$$

3. Results and discussions

The calculated results concerning the E1 ($\Delta L = 1, \Delta S = 0$) and the spin dipole ($\Delta L = 1, \Delta S = 1$) excitations for various Te isotopes are presented in this section. The Woods–Saxon potential with Chepurnov parametrisation is used as a single-particle basis [38]. The proton and neutron pairing gaps are determined as $\Delta_p = C_p/\sqrt{A}$ and $\Delta_n = C_n/\sqrt{A}$, respectively [39]. When the pairing strength parameters for ^{124,126}Te are chosen as $C_n = 6.0$ MeV and $C_p = 4.0$ MeV, the values of these parameters for ^{128,130}Te systems are $C_n = 7.0$ MeV, $C_p = 5.0$ MeV. The strength parameters for the isovector dipole–dipole interaction in E1 Hamiltonian and the effective spin-dipole interaction are determined as $\chi_1 = \chi_0 = 300A^{-5/3}$ MeV/fm^2. Energy-weighted sum rule obtained according to the formula

$$\sum_{j'j} E_{jj'}(\tau)[v^2_j(\tau) - v^2_{j'}(\tau)]\langle j' \| rY_1 \| j\rangle^2 = \frac{9}{4\pi}\frac{\hbar^2}{m}N_\tau$$

is fulfilled with a 1–2% accuracy. Here, v_j and N_τ are the single-particle amplitude with j quantum number and the particle number, respectively. The energy-weighted Thomas–Reiche–Kuhn (TRK) sum rule is obtained by summation over proton and neutron contributions with the proton and neutron effective charges, N/A and $-Z/A$, respectively,

$$S(\text{TRK}) = \frac{9}{4\pi}\frac{\hbar^2}{2m}\frac{NZ}{A}.$$

σ_0 is related to S(TRK) by

$$\sigma_0 = \frac{16\pi^3}{9\hbar c}e^2 S(\text{TRK}) = 60\frac{NZ}{A}(\text{MeV}\cdot\text{barn}).$$

The sum-rule values for σ_0 are 1.81, 1.83, 1.85 and 1.87 MeV·barn for $^{124-130}$Te, respectively.

The strength distributions for electric-dipole and spin-dipole transitions are given in figure 1. The right and left side figures represent E1 and spin-dipole excitations, respectively. As seen, most of the E1 transition strength is distributed over the energy region between 8 MeV$<\omega<$ 16 MeV. The centroid of the distribution for all isotopes is represented by a peak around 15 MeV. However, it can be said that the giant dipole resonance shows more fragmentation for heavy isotopes: The energy spectrum for ^{124}Te exhibits two important collective peaks at 14.77 and 15.24 MeV. Also, the giant dipole resonance region contains remarkable peaks at 12.76 MeV, 13.74 MeV and 16.05 MeV. The main configuration of the peak at 16.05 MeV is $(1g_{9/2} - 1h_{9/2})$p. The leading contribution of the peak at 13.74 MeV comes from $(1g_{9/2} - 2f_{7/2})$p and $(1f_{7/2} - 2d_{5/2})$p configurations.

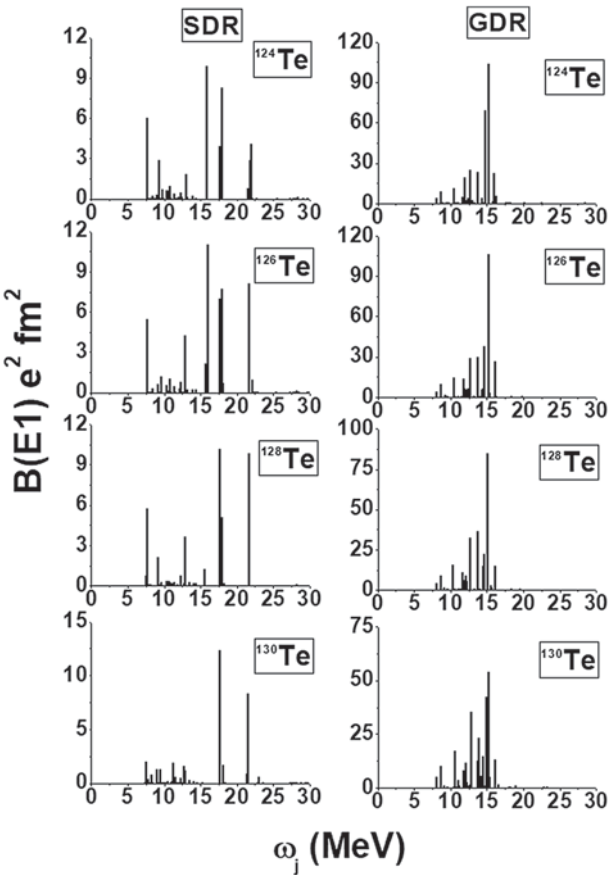

Figure 1. The electric-dipole and spin-dipole strength distributions for $^{124-130}$Te isotopes.

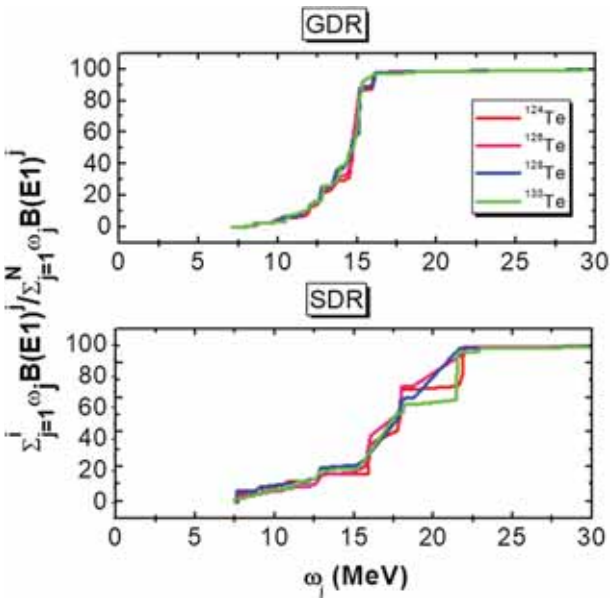

Figure 2. Energy-weighted strength distributions for electric-dipole and spin-dipole transitions.

The peak at 12.76 MeV is related to the collective E1 states. Nevertheless, the structure of the peaks obtained in the proton–proton spectra can also be influenced by neutron–neutron configurations due to the isovector part of the effective interaction. For instance, the structure of the peak at 16.05 MeV in the spectrum of ^{124}Te also contains a contribution of 4% coming from $(1h_{11/2} - 1i_{11/2})$n configuration. The energy spectrum for ^{126}Te shows a collective peak at 15.18 MeV. Moreover, there are considerable excitations at 10.41 MeV, 11.79 MeV, 12.75 MeV, 13.76 MeV, 14.70 MeV, 14.72 MeV and 16.10 MeV. The main configuration of the peak at 14.70 MeV is $(2d_{3/2} - 3p_{3/2})$p. The main contribution of the peak at 16.10 MeV comes from $(1g_{9/2} - 1h_{9/2})$p, $(2f_{7/2} - 2g_{9/2})$n and $(2d_{3/2} - 2f_{5/2})$p configurations. The other peaks in the giant dipole resonance region represent collective E1 states. The spectrum for ^{128}Te exhibits a maximum peak at 15.14 MeV which consists of many configurations. The structure of the peak at 16.08 MeV mainly consists of $(1g_{9/2} - 1h_{9/2})$p configuration. At the same time, the main configuration of the peak at 14.59 MeV is $(3s_{1/2} - 3p_{3/2})$p. The leading contribution of the peak at 13.78 MeV comes from $(1g_{9/2} - 2f_{7/2})$p and $(1f_{7/2} - 2d_{5/2})$p configurations. The dipole strength distribution for $A = 130$ isotope shows many peaks in the energy region of 10 MeV$< \omega <$ 15 MeV. The structure of the peak at 16.18 MeV mainly consists of $(1g_{9/2} - 1h_{9/2})$p configuration. The main configuration of the peak at 14.99 MeV is $(3s_{1/2} - 3p_{3/2})$p. At the same time, the leading contribution of the peak at 13.70 MeV comes from $(1g_{7/2} - 2f_{5/2})$p and $(1f_{7/2} - 2d_{5/2})$p configurations. Furthermore, it is clearly seen that the dipole transition strength for ^{130}Te shifts to the energies below 15 MeV. For all isotopes under consideration, the pigmy dipole resonance region contains two peaks around 8–9 MeV. The leading contribution for the peak with lower energy in the pigmy dipole resonance region comes from $(2p_{3/2} - 2d_{5/2})$p and $(1g_{9/2} - 1h_{11/2})$p configurations. The higher peak in this resonance region is related to the collective excitations. The energy spectrum for all isotopes shows no peak above 20 MeV. However, there are some excitations with low transition probability above 20 MeV. In figure 2, the distribution of total energy-weighted strength shows the existence of the contributions coming from a few excitations around 22.5 MeV.

The 1^- spin-dipole strength distribution exhibits important peaks for the isotopes under consideration. Nevertheless, it can be said that the 1^- spin dipole spectrum is fragmented in a wider energy range and the energy regions are more clearly separated from each other in comparison with the electric-dipole spectrum. Hence, the 1^- spin-dipole spectrum can be divided

into three different energy regions: (i) the pigmy spin-dipole resonance (PSDR) region ($0 < \omega < 10$ MeV), (ii) the giant spin-dipole resonance (GSDR) region (10 MeV $< \omega < 20$ MeV), (iii) the energy region ($\omega > 20$ MeV). The pigmy resonance region makes more contribution to the total strength compared to the same region in E1 distribution. For $A = 124$ isotope, when the structure of the peak at 7.73 MeV consists of $(1g_{9/2} - 1h_{11/2})$p configuration, the peak at 9.30 MeV has a more collective structure. There is a remarkable peak in the PSDR region of the energy spectrum for $A = 126$ isotope. The main configuration for the peak at 7.66 MeV is $(1g_{9/2} - 1h_{11/2})$p. For $A = 128$ isotope, there is a peak at 7.63 MeV which is mainly dominated by $(1g_{9/2} - 1h_{11/2})$p configuration. The other peak at 9.12 MeV has a collective structure. The PSDR region for $A = 130$ isotope includes the excited states which have collective structure. The second half of the GSDR region (15 MeV $< \omega < 20$ MeV) contains most of the strength belonging to this region. For ^{124}Te isotope, the GSDR includes a few significant peaks. The peak at 15.95 MeV consists of $(1g_{9/2} - 1h_{9/2})$p configuration. The main configuration for the peak at 17.60 MeV is $(1f_{7/2} - 1g_{7/2})$n. The leading contribution to the peak at 17.92 MeV comes from $(1f_{7/2} - 2d_{5/2})$n configuration. Also, the peak at 17.99 MeV is related to the collective spin-dipole excitations. The spin-dipole energy spectrum for ^{126}Te exhibits a maximum peak at 16.04 MeV. The structure of this peak completely consists of $(1g_{9/2} - 1h_{9/2})$p configuration. The leading contribution to the peak at 15.69 MeV comes from $(1h_{11/2} - 1i_{11/2})$n configuration. The second half of the GSDR region includes two important peaks at 17.69 MeV and 17.95 MeV. These two peaks show a collective structure over different configurations. The first half of the GSDR region (10 MeV $< \omega < 15$ MeV) contains a remarkable peak at 12.94 MeV which is dominated by $(1f_{7/2} - 1g_{7/2})$p configuration. The maximum of the spectrum for ^{128}Te exhibits a collective structure. The spectrum for this isotope shows another peak at 18.02 MeV. The main configuration for this peak is $(1f_{7/2} - 1g_{7/2})$n. Likewise, the first half of the GSDR region has a significant peak at 12.89 MeV. The leading contribution to this peak comes from $(1f_{7/2} - 1g_{7/2})$p configuration. For ^{130}Te isotope, the corresponding excited state in the first half of the GSDR region which is obtained at 12.94 MeV and 12.89 MeV for $A = 126$ and 128 isotopes, respectively is divided into two peaks at 12.72 MeV and 12.91 MeV. However, the second half of this energy region almost shows a single peak at 17.72 MeV which is dominated by $(1g_{9/2} - 1h_{9/2})$p configuration. Hence, it can be said that the spin-dipole transition strength in the first half of the GSDR region shifts to the second half of this region. Moreover, the energy region $\omega > 20$ MeV for all isotopes includes a single peak around 21.5–22 MeV. This single peak for $A = 128$ and 130 isotopes is related to the collective spin-dipole states. For $A = 126$ isotope, this peak is divided into two parts: The first part at 21.70 MeV has a collective structure and the leading configuration for the second part at 21.76 MeV is $(2s_{1/2} - 2p_{3/2})$p. For $A = 124$ isotope, the peak in this energy region is divided into three states at 21.85 MeV, 21.88 MeV and 21.91 MeV: The leading contribution to the state at 21.85 MeV comes from $(2s_{1/2} - 2p_{3/2})$p configuration. The main configuration for both states at 21.88 MeV and 21.91 MeV is $(2p_{3/2} - 3d_{5/2})$p.

The energy-weighted strength distributions (EWSD) in figure 2 confirm the comments mentioned above. As seen, the EWSD for E1 transitions shows variation in the energy region 8 MeV $< \omega < 16$ MeV. The present distributions in figure 2 confirm that the E1 excitations higher than 20 MeV have no remarkable contribution to the total energy-weighted strength. However, the EWSD for spin-dipole excitations shows a variation in a wider energy range in comparison with EWSD for E1 excitations.

A comparison of the calculated cross-sections and energies for E1 resonance with the corresponding experimental data [2–5] is presented in tables 1 and 2, respectively. For each isotope, the corresponding energies for the two important peaks and their percentage contributions to the total strength are given in the last two columns of table 2. As is seen, significant contributions to the total dipole strength come from the excitation energies close to the experimental energy. It can be said that the present σ_{-1} values show a good agreement with the experimental data. Also, the calculated σ_{-2} values for $A = 128, 130$ isotopes are in agreement with the experimental values. The present σ_{-2} values for $A = 124, 126$ isotopes are not far away from the corresponding experimental data. The calculated values for σ_0 cross-section are also given in table 1. The experimental σ_0 values for the isotopes under consideration are around 2 MeV·barn [40–45]. Hence, it can be said that the experimental σ_0 values are enhanced by about 10% compared to the corresponding sum-rule values. As the experimental dipole sum is usually enhanced compared to S(TRK) by about 50–100% in many nuclei, there is no need to emphasise an agreement with the TRK sum rule values. Note that S(TRK) is derived by double commutator of the kinetic energy term with the dipole operator, and the dipole sum agrees with S(TRK) only if the interaction commutes with the dipole operator. In general and in reality, the interaction does not commute with the operator. The contributions of the PDR and the PSDR strengths to the corresponding total strengths are shown in table 3. The

Table 1. The cross-section values for E1 resonance.

Isotopes	σ_{-2} (mb/MeV) (Exp)	σ_{-1} (Mb) (Exp)	σ_{-2} (mb/MeV)	σ_{-1} (Mb)	σ_0 (MeV·barn)
^{124}Te	8.4	128.0	9.62	132.66	1.88
^{126}Te	8.6	130.0	9.95	135.93	1.91
^{128}Te	9.1	135.0	9.71	131.35	1.83
^{130}Te	9.4	140.0	9.83	131.69	1.88

Table 2. The energy values for E1 resonance.

Isotopes	ω (MeV) (Exp)	ω (MeV)	Contribution (%)
^{124}Te	15.2	14.77,15.24	21.83,33.92
^{126}Te	15.1	14.72,15.18	11.62,34.01
^{128}Te	15.2	15.07,15.14	5.49,28.23
^{130}Te	15.1	14.99,15.17	13.65,17.49

Table 3. Percentage contributions of PDR and PSDR.

Isotopes	PDR (%)	PSDR (%)
^{124}Te	4.6	19.4
^{126}Te	4.9	14.0
^{128}Te	5.0	21.1
^{130}Te	5.1	15.8

second and third columns represent the PDR and PSDR contributions, respectively. It is clearly seen that PSDR contributes more to the corresponding total strength compared to PDR. When the PDR shows a negligible isotopic dependence, the PSDR exhibits a remarkable isotopic dependence. However, the PSDR contribution randomly changes for different isotopes. Hence, it is not possible to make a certain comment on the isotopic dependence of the PSDR.

4. Conclusion

The energy spectra of the 1^- excitations for ^{124,126,128,130}Te isotopes are calculated within the framework of (pp+nn) QRPA method. For E1 states ($\Delta L = 1, \Delta S = 0$), the broken translational invariance in the mean field level of approximation is restored by considering a separable isoscalar effective interaction within Pyatov's restoration method. Then, the restoration of broken Galilean invariance of pairing interaction is performed according to the same method. The E1 transition probabilities and energies are computed using the restored Hamiltonian and the energy spectra are obtained for the isotopes under consideration. Most of the total dipole strength is distributed over the energy range 8 MeV $< \omega <$ 16 MeV. The giant dipole resonance is obtained around 15 MeV. The dipole strength shifts to lower energies than 15 MeV for heavier isotopes. The microscopic structures of the peaks in the proton spectra can include the contributions coming from neutron–neutron configurations due to the isovector interaction term in the total Hamiltonian. Also, the calculated energies and cross-sections show a good agreement with the corresponding experimental data. The wave functions of the 1^- excitations in even–even nuclei can also be obtained by the spin-dipole interaction ($\Delta L = 1, \Delta S = 1$). The spin-dipole excitations are not related to any exact symmetry of nuclear Hamiltonian. Therefore, these excitations are obtained by including a schematic separable effective interaction. The effective interaction potential consists of isoscalar and isovector parts as seen in eq. (9). The isovector effects on spin-dipole spectra are clearly seen in the detailed analysis of the structures of the peaks. The fragmentation of the spin-dipole transition strength occurs in a wider energy range compared to E1 transitions. Hence, the spin-dipole spectrum consists of three energy regions: (i) Pigmy spin-dipole resonance, (ii) giant spin-dipole resonance, (iii) $\omega >$ 20 MeV. Unlike E1 transitions, the spin-dipole transition strength shifts to higher energies than 20 MeV for heavy isotopes. As a result, the following remarks can be summarised:

- The electric-dipole probabilities for open-shell Te isotopes are investigated within a translational and Galilean invariant model which was previously applied for deformed nuclei.
- The present calculations give a theoretical description of the charge-conserving spin-dipole 1^- excitations.

References

[1] J E Alam, *Pramana – J. Phys.* **84**, 861 (2015)
[2] D J Horen *et al*, *Phys. Lett. B* **99**, 383 (1981)
[3] X Yang *et al*, *Phys. Rev. C* **48**, 1158 (1993)
[4] K Pham *et al*, *Phys. Rev. C* **51**, 526 (1995)
[5] H Akimune *et al*, *Phys. Rev. C* **52**, 604 (1995)
[6] A Krasznahorkay *et al*, *Phys. Rev. Lett.* **82**, 3216 (1999)
[7] H Akimune *et al*, *Phys. Rev. C* **61**, 011304-1 (1999)
[8] S M Austin *et al*, arXiv:nucl-ex/0012005 (2000)
[9] A Krasznahorkay *et al*, *Phys. Rev. C* **64**, 067302 (2001)
[10] J Janecke *et al*, *Nucl. Phys. A* **687**, 270c (2001)
[11] L Stuhl *et al*, *J. Phys: Conf. Ser.* **381**, 012096-1 (2012)
[12] T Wakasa *et al*, *Phys. Rev. C* **85**, 064606-1 (2012)
[13] T Suzuki and H Sagawa, *Eur. Phys. J. A* **9**, 49 (2000)
[14] T Suzuki and H Sagawa, *Nucl. Phys. A* **718**, 446c (2003)
[15] E A Moukhai, V A Rodin and M H Urin, *Phys. Lett. B* **447**, 8 (1999)
[16] G A Lalazissis *et al*, *Phys. Rev. C* **71**, 024312-1 (2005)
[17] H Liang, N V Giai and J Meng, *Phys. Rev. Lett.* **101**, 122502 (2008)
[18] C L Biai *et al*, *Phys. Rev. C* **83**, 054316 (2011)
[19] T Kawabata *et al*, arXiv:nucl-ex/0202015 (2002)
[20] F T Baker *et al*, *Phys. Rev. C* **40**, 1877 (1989)
[21] F Osterfeld, *Rev. Mod. Phys.* **64**, 491 (1992)
[22] N I Pyatov and D I Salamov, *Nucleonica* **22**, 127 (1977)
[23] O Civitarese and M C Licciardo, *Phys. Rev. C* **38**, 967 (1988)
[24] O Civitarese and M C Licciardo, *Phys. Rev. C* **41**, 1778 (1990)
[25] H Sakamoto and T Kishimoto, *Nucl. Phys. A* **528**, 73 (1991)
[26] O Civitarese, A Faessler and M C Licciardo, *Nucl. Phys. A* **542**, 221 (1992)
[27] T Babacan *et al*, *J. Phys. G* **30**, 759 (2004)
[28] T Babacan, D I Salamov and A Kkbursa, *Phys. Rev. C* **71**, 037303-1 (2005)
[29] D I Salamov *et al*, *Pramana – J. Phys.* **66**, 1105 (2006)
[30] L Arisoy and S Unlu, *Nucl. Phys. A* **883**, 35 (2012)
[31] S Unlu and N Cakmak, *Nucl. Phys. A* **939**, 13 (2015)
[32] F A Gareev *et al*, *Sov. J. Nucl. Phys.* **33**, 645 (1981)
[33] E Guliyev *et al*, *Phys. Lett. B* **532**, 173 (2002)
[34] E Guliyev, A A Kuliev and F Ertugral, *Eur. Phys. J. A* **39**, 323 (2009)
[35] F Ertugral *et al*, *Cent. Eur. J. Phys. C* **7**, 731 (2009)
[36] H Quliyev *et al*, *Appl. Sci. Rep.* **14**, 199 (2016)
[37] N N Bogolyubov, JINR Rep. P-511, Dubna (1960)
[38] V G Soloviev, *Theory of complex nuclei* (Pergamon, New York, 1976)
[39] A A Bohr and B R Mottelson, *Nuclear structure* (W. A. Benjamin, Amsterdam, New York, 1969)
[40] B L Berman *et al*, *Phys. Rev.* **162**, 1098 (1967)
[41] A Lepretre *et al*, *Nucl. Phys. A* **175**, 609 (1971)
[42] S C Fultz *et al*, *Phys. Rev.* **186**, 1255 (1969)
[43] A Lepretre *et al*, *Nucl. Phys. A* **219**, 39 (1974)
[44] A Lepretre *et al*, *Nucl. Phys. A* **258**, 350 (1976)
[45] P Carlos *et al*, *Nucl. Phys. A* **225**, 171 (1974)